Quantum Error Correction with Superpositions of Squeezed Fock States

Yexiong Zeng,[1,2] Fernando Quijandría,[1] Clemens Gneiting,[1,*] and Franco Nori[1,3,†]

[1]*RIKEN Center for Quantum Computing, RIKEN, Wakoshi, Saitama 351-0198, Japan*

[2]*Key Laboratory of Low-Dimensional Quantum Structures and Quantum Control of Ministry of Education, Department of Physics and Synergetic Innovation Center for Quantum Effects and Applications, Hunan Normal University, Changsha 410081, China*

[3]*Quantum Research Institute and Department of Physics, University of Michigan, Ann Arbor, Michigan 48109-1040, USA*

(Received 23 September 2025; revised 4 March 2026; accepted 20 April 2026; published 15 May 2026)

Bosonic codes, leveraging infinite-dimensional Hilbert spaces for redundancy, offer great potential for encoding quantum information. However, a practical continuous-variable bosonic code that can simultaneously correct both photon loss and dephasing errors, while achieving a high level of compliance with the Knill-Laflamme conditions within an experimentally friendly structure, remains elusive. Here, we propose a code based on the superposition of squeezed Fock states with an error-correcting capability that scales as $\propto \exp(-7r)$, where r is the squeezing level. The codewords remain orthogonal at all squeezing levels. In particular, this code achieves high-precision error correction for both single-photon loss and dephasing, even at moderate squeezing levels. Building on this code, we develop quantum error correction schemes that exceed the breakeven point, supported by analytical derivations of all necessary quantum gates. Our code offers a competitive alternative to previous encodings for quantum computation using continuous bosonic qubits.

DOI: 10.1103/hr5f-lvy7

Introduction—Quantum states are fragile due to their high susceptibility to environmental noise, which poses a significant challenge to realizing quantum computation [1–7]. Quantum error correction (QEC), which restores quantum information degraded by noise channels through syndrome measurements or reservoir engineering, is therefore essential for fault-tolerant quantum computing [8–15]. This process requires encoding a single logical qubit redundantly in large Hilbert spaces, typically by employing a block of multiple physical qubits or a single higher-dimensional bosonic mode [16–21]. In particular, bosonic codes enable QEC at the level of a single bosonic mode with a well-defined set of dominant error channels [22–28]. While logical error rates cannot be arbitrarily suppressed in these architectures, concatenating bosonic codes with other error-correcting codes, such as the surface code, provides a promising route toward comprehensive error suppression and large-scale fault-tolerant quantum computation [29–31].

Bosonic codes hold promise for quantum information processing and thus have garnered considerable attention [32–35]. In many physical implementations of bosonic modes, single-photon loss and dephasing constitute the dominant noise channels, and bosonic codes are often designed to mitigate these errors [36–38]. The more the codewords are distributed across the Fock space (i.e., demanding increased coherence), the more dephasing becomes a significant noise source [39–41]. Various bosonic codes are designed to correct different types of errors and can be broadly classified into *continuous* and *discrete* codes. As in previous works [24,42], discrete bosonic codes encode logical states in superpositions over a *finite* set of Fock states, whereas continuous codes, such as cat and Gottesman-Kitaev-Preskill (GKP) codes [22,23,26], are supported on an unbounded set of Fock states.

Being a superposition of a finite number of Fock states, discrete bosonic codes exhibit a simple structure especially if they are tailored to correct a small number of errors. Nevertheless, this apparent simplicity does not translate into trivial schemes to prepare and control these states, as addressing a few Fock states requires a fine-tuned control of the quantum system. Moreover, continuous bosonic codes, such as the squeezed cat or the GKP code, might offer certain advantages for state preparation or control owing to their structure, which relies on displacement and squeezing operations that can be readily implemented in various quantum platforms, such as superconducting circuits, optical systems, and trapped ions [43–45]. Notably, this class of codes typically relies on codewords that are strictly not orthogonal, and therefore one needs to choose parameter regimes in which orthogonality is approximately satisfied. Despite some potential advantages in their structure as compared to their discrete counterparts, existing continuous bosonic codes are typically not tailored to

*Contact author: clemens.gneiting@riken.jp

†Contact author: fnori@riken.jp

simultaneously address single-photon loss and dephasing [33,34,40]. For example, squeezed cat codes are limited to correcting either single-photon loss or dephasing errors independently, while squeezed Fock codewords are inherently nonorthogonal and thus exhibit diminished performance, particularly at low squeezing levels [46–51]. Developing strictly orthogonal bosonic codes, capable of simultaneously correcting both photon loss and dephasing at experimentally feasible squeezing levels, is therefore essential for scalable bosonic quantum computing.

In this Letter, we combine the advantages of continuous and discrete bosonic codes to construct a strictly orthogonal code that achieves high-precision correction of both single-photon loss and dephasing noise. The proposed codewords are composed of tailored superpositions of squeezed Fock states, where the specific choice of superposition by construction ensures exact orthogonality of the codewords—at any squeezing level r. Meanwhile, the squeezing operation distributes the codewords continuously over the infinite-dimensional Fock space. Our analytical results demonstrate an exponential suppression of the infidelity scaling as $\exp(-7r)$ for combined photon loss and dephasing errors, outperforming all existing continuous bosonic codes. Therefore, the proposed code enables high-precision correction of both single-photon loss and dephasing errors at moderate squeezing levels. In addition, it facilitates straightforward implementation of logical qubit gates with experimentally accessible operations. Specifically, the code supports a simple, error-transparent logical Pauli-X gate that remains effective even within the error space. This property constitutes one of the main advantages of our code. Moreover, we analytically design effective quantum gates to implement both autonomous and parity-measurement-based quantum error correction protocols.

Codewords—We propose a novel continuous bosonic code that synthesizes discrete and continuous characteristics, specifically designed to correct single-photon loss and dephasing error channels in combination. The logical codewords are defined as

$$|0_L\rangle = \hat{S}(r)(\alpha|n+2\rangle - \beta|n\rangle),$$
$$|1_L\rangle = \hat{S}(-r)(\alpha|n+2\rangle + \beta|n\rangle) \tag{1}$$

where α ($|\beta|^2 + |\alpha|^2 = 1$) is determined by enforcing the orthogonality condition $\langle 0_\mathrm{L}|1_\mathrm{L}\rangle = 0$, $\hat{S}(r)$ denotes the squeezing operator with squeezing amplitude r, and $|n\rangle$ are the Fock states (n will be specified below).

To evaluate the QEC capability against single-photon loss and dephasing, we examine the Knill-Laflamme (KL) criterion for the error operator set $\mathbf{E} = \{\hat{I}, \hat{a}, \hat{n}, \hat{n}^2\}$ [46,49,50], where $\hat{a}$ and $\hat{n}$ are the annihilation and number operator, respectively. The KL criterion reads $\langle u_L|\hat{E}_i^\dagger \hat{E}_j|v_L\rangle = C_{ij}\delta_{uv}$ [52], where the C_{ij} form a Hermitian matrix, $\hat{E}_i, \hat{E}_j \in \mathbf{E}$ denote error operators, and $|u_L\rangle, |v_L\rangle \in \{|0_L\rangle, |1_L\rangle\}$ represent the codewords. Exact satisfaction of the KL condition is a prerequisite for complete error correction, and the degree of approximate fulfillment determines the maximal achievable fidelity [53–56]. We quantify the deviation from the KL condition using the indicator

$$K_{\mathrm{err}} = \sum_{ij} |M_{ij}^{00} - M_{ij}^{11}|^2 + |M_{ij}^{01}|^2, \tag{2}$$

where $M_{ij}^{\mu\nu} = \langle \mu_\mathrm{L}|\hat{E}_i^\dagger \hat{E}_j|\nu_\mathrm{L}\rangle$. A smaller value of K_{err} implies a closer approximation to the ideal KL condition and hence stronger error-correcting performance.

The condition $M_{ij}^{00} = M_{ij}^{11}$ is satisfied for the code in Eq. (1), and hence the first term in Eq. (2) vanishes identically. This indicates that the error process does not distinguish between logical basis states—a distinct advantage over the squeezed cat code. Consequently, only the off-diagonal terms quantifying the coherence between logical states affected by errors contribute to the deviation from the KL condition. Although some off-diagonal terms M_{ij}^{01} are nonzero, they remain exponentially small, scaling as $\sim e^{-7r}$ for odd n and $\sim e^{-5r}$ for even n. This difference arises from the distinct probability amplitude distributions of squeezed even and odd Fock states in Fock space. Since increasing n does not improve the scaling behavior but increases the average excitation number—which is approximately proportional to the error occurrence probability—we select $n = 1$ as the optimal choice and focus on it hereafter.

We simulate K_{err} in Fig. 1(a) for different values of n, confirming that $n = 1$ is the optimal choice and that the QEC performance improves with increasing squeezing. The nonzero terms responsible for the deviation from the KL condition can be approximately expanded in exponentials of the squeezing amplitude r,

$$\langle 1_L|\hat{n}^i|0_L\rangle = S_i e^{-7r} + \mathcal{O}(e^{-9r}), \quad i = 1, 2, 3, 4 \tag{3}$$

with $S_i \in \mathbf{S} = \{\pm 6.4\sqrt{3}, 3.2\sqrt{2}(5 \mp \sqrt{6}), 24\sqrt{2} \mp 36.8\sqrt{3}, 8\sqrt{2}(31 \pm 5\sqrt{6})\}$, where $\pm$ correspond to different solutions of α. The solutions for the coefficient α are not unique; however, this ambiguity does not affect the exponential scaling. Note that all other terms of the KL conditions are strictly satisfied. As we will detail next, the scaling of the off-diagonal terms in K_{err} achieved by our proposed code represents a significant improvement over previous continuous bosonic codes.

The value of K_{err} reaches the order of 10^{-2} at $r \approx 0.921$ (approximately 8 dB), a squeezing level readily achievable in current experiments [47]. For the error set $\mathbf{E}$, this corresponds to a reduction in deviation by more than *three* and *two* orders of magnitude compared to the squeezed cat and squeezed Fock codes, respectively. This performance gap stems from the substantial overlap of squeezed cat

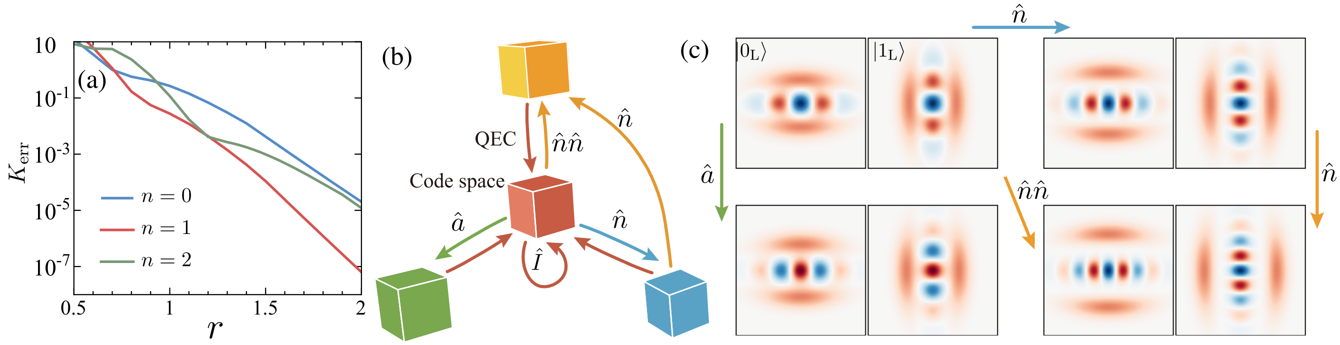

FIG. 1. (a) Deviation from the KL condition versus the squeezing amplitude r for different values of n. An exponential decay is observed, with $n = 1$ exhibiting the best performance at large r. (b) Errors from the set $[\hat{I}, \hat{a}, \hat{n}, \hat{n}^2]$ acting on the logical subspace define the corresponding error spaces. The code and error spaces approximately satisfy the KL condition $K_{\rm err}$, enabling recovery via QEC. (c) Wigner functions of the codewords (related by a $\pi/2$ rotation) and associated error states (also related by a $\pi/2$ rotation) at 8 dB squeezing ($r \approx 0.921$). As the $\hat{n}$ and $\hat{n}^2$ operators do not affect the parity of the codewords (as compared to $\hat{a}$), the resulting error states have nonzero overlap with the codewords and with each other. This, in turn, is the reason for the nonvanishing deviation of the KL condition [cf. Eq. (3)].

codewords under the combined action of $\hat{a}$ and $\hat{n}^m$. Consequently, the code performs significantly worse for error sets that simultaneously include both operators, such as $\mathbf{E}$, even though subsets like $\{\hat{I}, \hat{a}\}$ or $\{\hat{I}, \hat{n}, \hat{n}^2\}$ remain approximately correctable. Similarly, the squeezed Fock code suffers from inherent nonorthogonality and off-diagonal terms M_{ij}^{01} that decay no faster than $\sim e^{-3r}$, resulting in markedly inferior error suppression relative to our code.

Short-time quantum dynamics gives rise to three distinct error subspaces, whose relation to the code space is depicted in Fig. 1(b). The corresponding Wigner functions of the codewords related by a $\pi/2$ rotation and their error-transformed states, are shown in Fig. 1(c). Consequently, the logical Pauli X operator is given by $\hat{X}_L = \exp[-i(\pi/2)\hat{n}]$, which remains effective within the error spaces; hence, it is an error-transparent gate. Furthermore, the Pauli-Z operator can be implemented as $\hat{Z}_L = \exp[-i\hat{H}_z(\hat{a}, \hat{a}^\dagger)]$, where $\hat{H}_z$ is expressed as a power-series expansion in the operators $\hat{a}$ and $\hat{a}^\dagger$ [46]. Finally, the algebraic properties of the Pauli operators and the structure of the codewords allow for a simplified preparation scheme—once one codeword is prepared, the other can be obtained through a rotational operation.

Error correction schemes—The strong alignment of the code with the KL conditions, together with the odd parity structure of the code space, enables the systematic design of QEC schemes by using an ancilla three-level system, as shown in Fig. 2(a), including both stroboscopic autonomous and parity-measurement-based approaches. Note that stroboscopic autonomous QEC proceeds via deterministically triggered recovery operations, unlike continuous autonomous QEC based on engineered dissipation. The encoded bosonic mode first undergoes a noise channel $\mathcal{E}(\cdot)$, followed by a recovery operation $\mathcal{R}(\cdot)$. For a short evolution time τ, the combined effect of single-photon loss and dephasing is described by a Kraus expansion, $\mathcal{E}[\hat{\rho}] \approx \sum_{i=1}^{3} \hat{A}_i \hat{\rho} \hat{A}_i^\dagger$, where the Kraus operators are given by $\hat{A}_1 \approx \hat{I} - (\kappa\tau/2)\hat{n} - (\kappa_\phi \tau/2)\hat{n}^2$, $\hat{A}_2 \approx \sqrt{\kappa_\phi \tau}\hat{n}$, and $\hat{A}_3 \approx \sqrt{\kappa\tau}\hat{a}$ [46]. Here, κ and κ_ϕ are the single-photon loss and

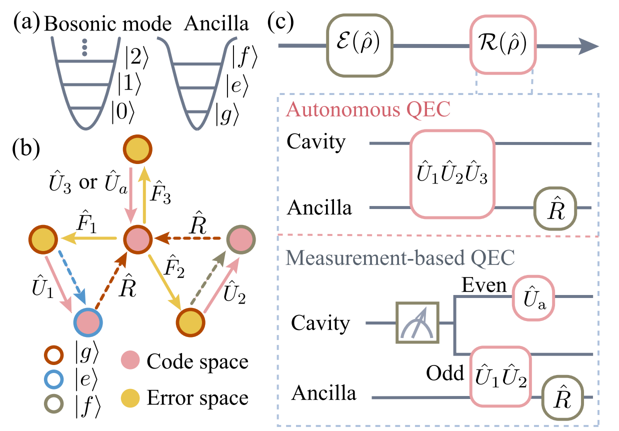

FIG. 2. (a) The encoded bosonic mode resides in an infinite-dimensional Hilbert space, while the auxiliary system is a discrete-level system, such as a qutrit. (b) The bosonic mode is initialized in an encoded state $|\psi_{\rm L}\rangle$, and the auxiliary system in its ground state $|g\rangle$. Noise operators $\hat{F}_i$, derived from the error set $\mathbf{E}$, map the code space into approximately orthogonal error subspaces. Control operations $\hat{U}_i$ conditionally restore the encoded state while exciting the auxiliary system. A reset operation $\hat{R}$ returns the auxiliary system to $|g\rangle$, completing a QEC cycle. (c) After the error channel $\mathcal{E}(\cdot)$, two alternative recovery schemes $\mathcal{R}(\cdot)$ are considered. The stroboscopic autonomous QEC completes the recovery without measurements, while the measurement-based protocol uses a parity measurement to identify the error: even parity invokes $\hat{U}_a$ [Eq. (S23)] for direct recovery, odd parity triggers a two-step correction via $\hat{U}_1$ and $\hat{U}_2$. Iterating these cycles enables long-term protection of encoded quantum information.

dephasing rates, respectively. To construct the QEC channel, we diagonalize the symmetric matrix $\boldsymbol{J} = V\boldsymbol{\Lambda}V^\dagger$, with elements $J_{ij} = \langle u_L|\hat{A}_i^\dagger \hat{A}_j|u_L\rangle$. The noise channel can be recast as $\mathcal{E}[\hat{\rho}] \approx \sum_i \hat{F}_i\hat{\rho}\hat{F}_i^\dagger$, where the transformed Kraus operators are [53]

$$\hat{F}_i = \sum_{k=1}^{3} V_{ki}\hat{A}_k, \quad i = 1, 2, 3. \tag{4}$$

These operators satisfy $\hat{P}_L\hat{F}_i^\dagger\hat{F}_j\hat{P}_L \approx \Lambda_{ij}\delta_{ij}\hat{P}_L$, where $\hat{P}_L$ denotes the projector onto the code space. This ensures that the $\hat{F}_i$ operators map the code space onto orthogonal error subspaces, enabling efficient recovery.

As shown in Figs. 2(a) and 2(b), we couple the encoded bosonic mode to an ancillary qutrit initialized in its ground state $|g\rangle$ to identify and correct the errors $\hat{F}_i$, resulting in the initial joint state $|\psi_\mathrm{L}, g\rangle$. A sequence of unitary operations $\hat{U}_i$ [$i = 1$, 2, 3 in Eq. (6) and $i = a$ in Eq. (S23)] is then applied to coherently restore the system to the code space. Since only $\hat{a}$ flips the parity of the encoded state, the respective error syndrome can be extracted via a parity measurement: based on the measurement outcome, we apply $\hat{U}_a$ for the parity-flip case or the common recovery $\hat{U}_2\hat{U}_1$ otherwise, followed by the Hermitian operation $\hat{R}$ that coherently returns the qutrit to the ground state $|g\rangle$ without inducing excitations, as shown in Fig. 2(c). While conceptually similar to the autonomous scheme, the measurement-based approach requires active readout and feedforward, introducing additional overhead in experimental implementations. We therefore focus on the stroboscopic autonomous scheme in the main text, with the measurement-based protocol detailed in [46].

The recovery unitary operations $\hat{U}_i$ correct errors associated with the operators $\hat{F}_i$ while acting as the identity operator in the other orthogonal error subspaces. As a result, they do not interfere with errors arising from other Kraus operators. Following the recovery process, the encoded state $|\psi_L\rangle$ is approximately restored, while the ancilla qutrit transitions to different states depending on the specific error that occurred [46]. Finally, the ancilla qutrit is rapidly reset to its ground state via a strongly dissipative interaction R with a reservoir, completing the QEC cycle without measurement and thereby enabling autonomous QEC. The entire QEC cycle can be described by the following equation

$$\mathcal{R}_\mathrm{a} \circ \mathcal{E}[\hat{\rho}_L] = R\big[\hat{U}\mathcal{E}[\hat{\rho}_\mathrm{L}] \otimes |g\rangle\langle g|\hat{U}^\dagger\big] \approx \hat{\rho}_L \otimes |g\rangle\langle g|, \tag{5}$$

where $\mathcal{R}_\mathrm{a}$ is the autonomous QEC channel, $\hat{U} = \hat{U}_3\hat{U}_2\hat{U}_1$, $\hat{\rho}_L$ is the encoded state $\hat{\rho}_L = |\psi_L\rangle\langle\psi_L|$, and R stands for the reset of the ancilla qutrit to its ground state.

Here, we present an analytical approach for the above recovery unitary operations by incorporating an ancilla qutrit system, with the detailed expressions given by

$$\begin{aligned} \hat{U}_1 &= \hat{L}_1|e\rangle\langle g| + \hat{L}_1^\dagger|g\rangle\langle e| + \hat{U}_{1,\mathrm{re}}, \\ \hat{U}_2 &= \hat{L}_2|f\rangle\langle g| + \hat{L}_2^\dagger|g\rangle\langle f| + \hat{U}_{2,\mathrm{re}}, \\ \hat{U}_3 &= \big(\hat{L}_3 + \hat{L}_3^\dagger + \hat{I} - \hat{P}_L - \hat{P}_{F_3}\big)|g\rangle\langle g| + \hat{U}_{3,\mathrm{re}}, \end{aligned} \tag{6}$$

where $|e\rangle$, $|f\rangle$ are two excited states used to discriminate between different types of errors, the operator $\hat{L}_i = |0_L\rangle\langle 0_{F_i}| + |1_L\rangle\langle 1_{F_i}|$ is designed to recover information from the error space into the code space ($|u_{F_i}\rangle = \hat{F}_i|u_L\rangle/\|\hat{F}_i|u_L\rangle\|$), $\hat{P}_{F_i}$ is the projector operator of the i th error space, and $\hat{U}_{i,\mathrm{re}}$ supplements $\hat{U}_i$ to ensure it forms a unitary operator and leaves the recovered information unaffected ($\hat{U}_{i,\mathrm{re}}$ is provided in [46]). These unitary operations correct the corresponding errors without affecting other parts of the error space or states corrected after other errors occur. The availability of analytic expressions for the recovery unitaries (6) allows for their efficient implementation using well-established quantum control techniques, such as gradient ascent pulse engineering and machine-learning-based optimization [57–63]. Alternatively, we could use two-qubit or multilevel ancilla systems to design these unitary operations with the construction methodology similar to that of the qutrit ancilla system [46]. In principle, arbitrary unitary operations on the system can be achieved through optimal control techniques. As an example, we consider a superconducting cavity coupled to a transmon, where the composite gate $\hat{U}$ is realized by controlling the quadratures $\hat{x}$ and $\hat{p}$ of the bosonic mode, achieving a fidelity exceeding 0.99 [46]. The control fields can be flexibly adjusted to enhance the performance further, but such refinements are beyond the scope of this work.

Figure 3 shows the average infidelity versus the squeezing amplitude r and the dimensionless time scale $\kappa\tau$, where τ is the idle time and the fidelity is averaged over the six Pauli eigenstates [64]. For $r \gtrsim 0.8$ (corresponding to $\gtrsim$6.95 dB of squeezing), the autonomous QEC protocol can yield a gain $(1 - \bar{F}_\mathrm{be})/(1 - \bar{F}_\mathrm{auto}) > 100$ for $\kappa/\kappa_\phi \approx 5.5$ and $\kappa/\kappa_\phi \approx 2.5$, as shown in Figs. 3(a) and 3(b) (respectively). Here, $\bar{F}_\mathrm{be}$ denotes the channel fidelity of a qubit encoded in the bare Fock states $|0\rangle$ and $|1\rangle$ without QEC, while $\bar{F}_\mathrm{auto}$ corresponds to the autonomous QEC channel fidelity under the assumption of instantaneous recovery operations $\hat{U}_i$ (6). Our results show that moderate squeezing is required for a gain > 1, as the KL enhancement must outweigh the increased average photon number of the codewords. Notably, for amplitude r slightly above 0.8, the gain exceeds 1 for arbitrarily small $\kappa\tau$, as the KL contribution dominates over the excitations. Importantly, we simulate the full noise channel corresponding to photon-loss and dephasing noise. Only in the small time limit ($\kappa\tau, \kappa_\phi\tau \ll 1$), this channel can be approximated

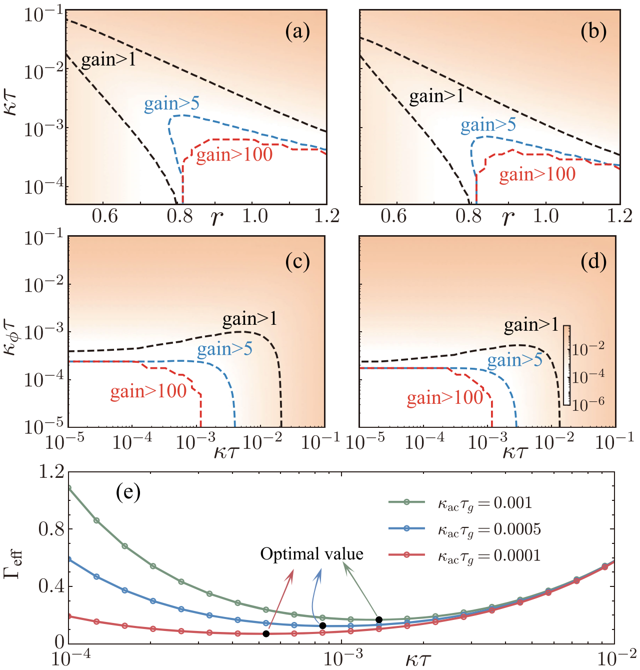

FIG. 3. Panels (a) and (b) show the channel infidelity per QEC cycle versus the dimensionless time scale $\kappa\tau$ and squeezing amplitude r for photon-loss–to–dephasing rate ratios $\kappa/\kappa_\phi \approx 5.5$ and 2.5, respectively. Panels (c) and (d) show the channel infidelity versus the single-photon loss and dephasing rates for $r = 0.9$ and $r = 1.0$. (e) Effective decay rate $\Gamma_{\rm eff}$ of the channel fidelity versus the idling time $\kappa\tau$ for different gate-time scales $\kappa_{ac}\tau_g$ at $r = 0.9$. All results are obtained by simulating the full master equation.

by the error set $\mathbf{E} = \{\hat{I}, \hat{a}, \hat{n}, \hat{n}^2\}$. Beyond this limit, the channel can induce cumulative error processes that are not accounted for by our code. Within the explored parameter regime, the optimal performance occurs around $r = 0.9$, which remains effective over a broad range of κ/κ_ϕ and outperforms stronger squeezing ($r = 1$), as shown in Figs. 3(c) and 3(d). Using a near-optimal recovery channel, such as the Petz recovery map [65,66], efficient error correction persists down to $r = 0.6$, with a gain exceeding 10 at $r = 0.6$ and $\kappa\tau = \kappa_\phi\tau \approx 0.01$ [46]. At the corresponding squeezing levels and time scales, the resulting infidelity is lower than that of both the squeezed cat code and the GKP code [39,40,64].

Finally, we assess ancilla errors on the channel fidelity by implementing the operations $\hat{U}_i$ using gates of finite duration. We further analyze the effect of ancilla decay $\kappa_{\rm ac}$ by extracting the effective decay rate of the channel fidelity, $\Gamma_{\rm eff} \propto -\ln[\bar{F}_{\rm auto}(\tau_{\rm al})]/\tau_{\rm al}$, as shown in Fig. 3(e), where $\tau_{\rm al} = \tau + \tau_g$ is the duration of a single QEC cycle. Here, we model the ancilla as a decaying mode $\hat{b}$ and incorporate the unitary process $\hat{U}_3\hat{U}_2\hat{U}_1 = \exp(-\hat{H}_{\rm eff}\tau_g)$ into the system dynamics with the effective Hamiltonian $\hat{H}_{\rm eff}$. For a fixed squeezing amplitude r, shorter gate times τ_g result in improved QEC performance. Moreover, ancilla dissipation leads to the emergence of an optimal idle time. For $r = 0.9$, the optimal idle time is on the order of 10^{-3}, consistent with the experimentally optimal time for implementing GKP encoding ($\kappa\tau \approx 0.00074$), and the corresponding gate times fall within experimentally achievable regimes [67]. For these optimal idle-time scales, the gain exceeds 5, comparable to the case where the noise of the ancillary qubit is neglected. Requiring significantly less squeezing while supporting realistic idling times τ, our code achieves high QEC performance and is compatible with a wide range of experimental platforms, including trapped ions, optical systems, and 3D superconducting microwave cavities [67–76].

We emphasize that binomial codes can be designed to satisfy the KL conditions for the same error set as our proposed code. The result is a high-order code involving superpositions up to Fock state $|10\rangle$. Whereas these codes offer an error correction performance comparable to ours, they are experimentally challenging due to their reliance on multiple high-Fock components [24]. So far, experiments have only realized the lowest-order binomial code with superpositions up to Fock state $|4\rangle$, which are limited to correcting single-photon loss [77]. In contrast, encodings within low-Fock subspaces such as Fock states $|1\rangle$ and $|3\rangle$ are well established experimentally [78–80]. Our code builds on this subspace, requiring only an additional squeezing operation for codeword preparation. This results in a preparation process that is experimentally more accessible—even simpler than that of the lowest-order binomial codes—while offering enhanced error correction. Consequently, our code combines improved performance with high experimental feasibility.

Conclusion—We introduced a squeezed bosonic code that robustly corrects for both single-photon loss and dephasing in continuous-variable quantum systems under experimentally feasible conditions. Exploiting the infinite-dimensional Hilbert space of bosonic modes, our code features error-correcting capabilities that scale exponentially with the squeezing amplitude [$\propto \exp(-7r)$] while maintaining orthogonal codewords at all squeezing levels. As a result, the QEC performance improves exponentially with the squeezing for the error set $\mathbf{E}$, enabling high QEC efficiency at relatively low squeezing. Moreover, the code applies equally when $\hat{a}$ is replaced by $\hat{a}^\dagger$, which satisfies the same error-correction conditions. Building on this framework, we developed measurement-based and autonomous QEC protocols and provided an analytical description of the required recovery operations. Our analysis establishes that these QEC schemes can be implemented in a bosonic mode coupled to a qutrit. In conclusion, this new code represents a substantial advancement over previous continuous-variable bosonic qubit encodings for quantum computation.

Acknowledgments—F. N. is supported in part by the Japan Science and Technology Agency (JST) [via the CREST Quantum Frontiers program Grant No. JPMJCR24I2, the Quantum Leap Flagship Program (Q-LEAP), the Moonshot R&D Grant No. JPMJMS256E, and the ASPIRE program (Grant No. JPMJAP2513)], and the Office of Naval Research (ONR) Global (via Grant No. N62909-23-1-2074). C. G. was partly supported by RIKEN Incentive Research Projects.

Data availability—The data supporting the findings of this study are available from the author upon reasonable request.

[1] J. Chiaverini, D. Leibfried, T. Schaetz, M. D. Barrett, R. B. Blakestad, J. Britton, W. M. Itano, J. D. Jost, E. Knill, C. Langer, R. Ozeri, and D. J. Wineland, Realization of quantum error correction, Nature (London) **432**, 602 (2004).

[2] P. Schindler, J. T. Barreiro, T. Monz, V. Nebendahl, D. Nigg, M. Chwalla, M. Hennrich, and R. Blatt, Experimental repetitive quantum error correction, Science **332**, 1059 (2011).

[3] H. Mabuchi and P. Zoller, Inversion of quantum jumps in quantum optical systems under continuous observation, Phys. Rev. Lett. **76**, 3108 (1996).

[4] Google Quantum AI, Suppressing quantum errors by scaling a surface code logical qubit, Nature (London) **614**, 676 (2023).

[5] Google Quantum AI and Collaborators, Quantum error correction below the surface code threshold, Nature (London) **638**, 920 (2025).

[6] D. A. Lidar and T. A. Brun, *Quantum Error Correction* (Cambridge University Press, Cambridge, England, 2013).

[7] F. Gaitan, *Quantum Error Correction and Fault Tolerant Quantum Computing* (Taylor & Francis, Andover, England, 2018).

[8] J. Kerckhoff, H. I. Nurdin, D. S. Pavlichin, and H. Mabuchi, Designing quantum memories with embedded control: Photonic circuits for autonomous quantum error correction, Phys. Rev. Lett. **105**, 040502 (2010).

[9] B. M. Terhal, Quantum error correction for quantum memories, Rev. Mod. Phys. **87**, 307 (2015).

[10] R. L. Kosut, A. Shabani, and D. A. Lidar, Robust quantum error correction via convex optimization, Phys. Rev. Lett. **100**, 020502 (2008).

[11] J. P. Barnes and W. S. Warren, Automatic quantum error correction, Phys. Rev. Lett. **85**, 856 (2000).

[12] M. Sarovar and G. J. Milburn, Continuous quantum error correction by cooling, Phys. Rev. A **72**, 012306 (2005).

[13] J. Cohen and M. Mirrahimi, Dissipation-induced continuous quantum error correction for superconducting circuits, Phys. Rev. A **90**, 062344 (2014).

[14] G. Sarma and H. Mabuchi, Gauge subsystems, separability and robustness in autonomous quantum memories, New J. Phys. **15**, 035014 (2013).

[15] Y. Zeng, Z.-Y. Zhou, E. Rinaldi, C. Gneiting, and F. Nori, Approximate autonomous quantum error correction with reinforcement learning, Phys. Rev. Lett. **131**, 050601 (2023).

[16] A. Eickbusch, M. McEwen, V. Sivak, A. Bourassa, J. Atalaya *et al.*, Demonstration of dynamic surface codes, Nat. Phys. **21**, 1994 (2025).

[17] R. Dahan, G. Baranes, A. Gorlach, R. Ruimy, N. Rivera, and I. Kaminer, Creation of optical cat and GKP states using shaped free electrons, Phys. Rev. X **13**, 031001 (2023).

[18] C. Ryan-Anderson, J. G. Bohnet, K. Lee, D. Gresh, A. Hankin *et al.*, Realization of real-time fault-tolerant quantum error correction, Phys. Rev. X **11**, 041058 (2021).

[19] T. Matsuura, H. Yamasaki, and M. Koashi, Equivalence of approximate Gottesman-Kitaev-Preskill codes, Phys. Rev. A **102**, 032408 (2020).

[20] K. Fukui, T. Matsuura, and N. C. Menicucci, Efficient concatenated bosonic code for additive Gaussian noise, Phys. Rev. Lett. **131**, 170603 (2023).

[21] T. Hillmann, F. Quijandría, A. L. Grimsmo, and G. Ferrini, Performance of teleportation-based error-correction circuits for bosonic codes with noisy measurements, PRX Quantum **3**, 020334 (2022).

[22] D. Gottesman, A. Kitaev, and J. Preskill, Encoding a qubit in an oscillator, Phys. Rev. A **64**, 012310 (2001).

[23] M. Mirrahimi, Cat-qubits for quantum computation, C.R. Phys. **17**, 778 (2016).

[24] M. H. Michael, M. Silveri, R. T. Brierley, V. V. Albert, J. Salmilehto, L. Jiang, and S. M. Girvin, New class of quantum error-correcting codes for a bosonic mode, Phys. Rev. X **6**, 031006 (2016).

[25] V. V. Albert, K. Noh, K. Duivenvoorden *et al.*, Performance and structure of single-mode bosonic codes, Phys. Rev. A **97**, 032346 (2018).

[26] K. Fukui, A. Tomita, and A. Okamoto, Analog quantum error correction with encoding a qubit into an oscillator, Phys. Rev. Lett. **119**, 180507 (2017).

[27] R. Lescanne, M. Villiers, T. Peronnin, A. Sarlette, M. Delbecq, B. Huard, T. Kontos, M. Mirrahimi, and Z. Leghtas, Exponential suppression of bit-flips in a qubit encoded in an oscillator, Nat. Phys. **16**, 509 (2020).

[28] Y. Zheng, A. Ferraro, A. F. Kockum, and G. Ferrini, Gaussian conversion protocol for heralded generation of generalized Gottesman-Kitaev-Preskill states, Phys. Rev. A **108**, 012603 (2023).

[29] H. Putterman, K. Noh, C. T. Hann, G. S. MacCabe, S. Aghaeimeibodi *et al.*, Hardware-efficient quantum error correction via concatenated bosonic qubits, Nature (London) **638**, 927 (2025).

[30] K. Noh and C. Chamberland, Fault-tolerant bosonic quantum error correction with the surface–Gottesman-Kitaev-Preskill code, Phys. Rev. A **101**, 012316 (2020).

[31] D. Ruiz, J. Guillaud, A. Leverrier, M. Mirrahimi, and C. Vuillot, LDPC-cat codes for low-overhead quantum computing in 2D, Nat. Commun. **16**, 1040 (2025).

[32] W. Cai, Y. Ma, W. Wang, C.-L. Zou, and L. Sun, Bosonic quantum error correction codes in superconducting quantum circuits, Fundam. Res. **1**, 50 (2021).

[33] B. M. Terhal, J. Conrad, and C. Vuillot, Towards scalable bosonic quantum error correction, Quantum Sci. Technol. **5**, 043001 (2020).

[34] A. Joshi, K. Noh, and Y. Y. Gao, Quantum information processing with bosonic qubits in circuit QED, Quantum Sci. Technol. **6**, 033001 (2021).

[35] K. S. Chou, J. Z. Blumoff, C. S. Wang, P. C. Reinhold, C. J. Axline, Y. Y. Gao, L. Frunzio, M. H. Devoret, L. Jiang, and R. J. Schoelkopf, Deterministic teleportation of a quantum gate between two logical qubits, Nature (London) **561**, 368 (2018).

[36] P. Leviant, Q. Xu, L. Jiang, and S. Rosenblum, Quantum capacity and codes for the bosonic loss-dephasing channel, Quantum **6**, 821 (2022).

[37] L. Lami and M. M. Wilde, Exact solution for the quantum and private capacities of bosonic dephasing channels, Nat. Photonics **17**, 525 (2023).

[38] A. L. Grimsmo, J. Combes, and B. Q. Baragiola, Quantum computing with rotation-symmetric bosonic codes, Phys. Rev. X **10**, 011058 (2020).

[39] A. L. Grimsmo and S. Puri, Quantum error correction with the Gottesman-Kitaev-Preskill code, PRX Quantum **2**, 020101 (2021).

[40] D. S. Schlegel, F. Minganti, and V. Savona, Quantum error correction using squeezed Schrödinger cat states, Phys. Rev. A **106**, 022431 (2022).

[41] Y. Zeng, W. Qin, Y.-H. Chen, C. Gneiting, and F. Nori, Neural-network-based design of approximate Gottesman-Kitaev-Preskill code, Phys. Rev. Lett. **134**, 060601 (2025).

[42] Z. Ni, S. Li, X. Deng, Y. Cai, L. Zhang *et al.*, Beating the break-even point with a discrete-variable-encoded logical qubit, Nature (London) **616**, 56 (2023).

[43] P. Campagne-Ibarcq, A. Eickbusch, S. Touzard, E. Zalys-Geller, N. E. Frattini *et al.*, Quantum error correction of a qubit encoded in grid states of an oscillator, Nature (London) **584**, 368 (2020).

[44] C. Flühmann, T. L. Nguyen, M. Marinelli, V. Negnevitsky, K. Mehta, and J. P. Home, Encoding a qubit in a trapped-ion mechanical oscillator, Nature (London) **566**, 513 (2019).

[45] J. Hastrup and U. L. Andersen, Protocol for generating optical Gottesman-Kitaev-Preskill states with cavity QED, Phys. Rev. Lett. **128**, 170503 (2022).

[46] See Supplemental Material at http://link.aps.org/supplemental/10.1103/hr5f-lvy7 for details of the QEC process and explicit quantum-gate expressions.

[47] X. Pan, J. Schwinger, N.-N. Huang, P. Song, W. Chua, F. Hanamura, A. Joshi, F. Valadares, R. Filip, and Y. Y. Gao, Protecting the quantum interference of cat states by phase-space compression, Phys. Rev. X **13**, 021004 (2023).

[48] E. N. Bashmakova, S. B. Korolev, and T. Yu. Golubeva, Bosonic quantum error correction using squeezed Fock states, Phys. Rev. A **112**, 032434 (2025).

[49] T. Hillmann and F. Quijandría, Quantum error correction with dissipatively stabilized squeezed-cat qubits, Phys. Rev. A **107**, 032423 (2023).

[50] S. B. Korolev, E. N. Bashmakova, and T. Yu. Golubeva, Error correction using squeezed Fock states, Quantum Inf. Process. **23**, 354 (2024).

[51] L. Albano, D. F. Mundarain, and J. Stephany, On the squeezed number states and their phase space representations, J. Opt. B: Quantum Semiclassical Opt. **4**, 352 (2002).

[52] E. Knill, R. Laflamme, and L. Viola, Theory of quantum error correction for general noise, Phys. Rev. Lett. **84**, 2525 (2000).

[53] S. M. Girvin, Introduction to quantum error correction and fault tolerance, SciPost Phys. Lect. Notes, **070** (2023).

[54] D. W. Leung, M. A. Nielsen, I. L. Chuang, and Y. Yamamoto, Approximate quantum error correction can lead to better codes, Phys. Rev. A **56**, 2567 (1997).

[55] E. Knill and R. Laflamme, Theory of quantum error-correcting codes, Phys. Rev. A **55**, 900 (1997).

[56] P. Faist, S. Nezami, V. V. Albert, G. Salton, F. Pastawski, P. Hayden, and J. Preskill, Continuous symmetries and approximate quantum error correction, Phys. Rev. X **10**, 041018 (2020).

[57] N. Khaneja, T. Reiss, C. Kehlet, T. Schulte-Herbrüggen, and S. J. Glaser, Optimal control of coupled spin dynamics: Design of NMR pulse sequences by gradient ascent algorithms, J. Magn. Reson. **172**, 296 (2005).

[58] P. de Fouquieres, S. G. Schirmer, S. J. Glaser, and I. Kuprov, Second order gradient ascent pulse engineering, J. Magn. Reson. **212**, 412 (2011).

[59] J. R. Johansson, P. D. Nation, and F. Nori, QuTiP: An open-source Python framework for the dynamics of open quantum systems, Comput. Phys. Commun. **183**, 1760 (2012).

[60] A. Mercurio, Y.-T. Huang, L.-X. Cai, Y.-N. Chen, V. Savona, and F. Nori, QuantumToolbox.jl: An efficient Julia framework for simulating open quantum systems, Quantum **9**, 1866 (2025).

[61] J. R. Johansson, P. D. Nation, and F. Nori, QuTiP 2: A Python framework for the dynamics of open quantum systems, Comput. Phys. Commun. **184**, 1234 (2013).

[62] N. Lambert, E. Giguère, P. Menczel *et al.*, QuTiP 5: The quantum toolbox in Python, Phys. Rep. **1153**, 1 (2026).

[63] A. Eickbusch, V. Sivak, A. Z. Ding, S. S. Elder, S. R. Jha, J. Venkatraman, B. Royer, S. M. Girvin, R. J. Schoelkopf, and M. H. Devoret, Fast universal control of an oscillator with weak dispersive coupling to a qubit, Nat. Phys. **18**, 1464 (2022).

[64] B. Royer, S. Singh, and S. M. Girvin, Stabilization of finite-energy Gottesman-Kitaev-Preskill States, Phys. Rev. Lett. **125**, 260509 (2020).

[65] H. Kwon, R. Mukherjee, and M. S. Kim, Reversing Lindblad dynamics via continuous Petz recovery map, Phys. Rev. Lett. **128**, 020403 (2022).

[66] B. Li, Z. Wang, G. Zheng, Y. Wong, and L. Jiang, Optimality condition for the Petz map, Phys. Rev. Lett. **134**, 200602 (2025).

[67] V. V. Sivak, A. Eickbusch, B. Royer *et al.*, Real-time quantum error correction beyond break-even, Nature (London) **616**, 50 (2023).

[68] B. de Neeve, T.-L. Nguyen, T. Behrle, and J. P. Home, Error correction of a logical grid state qubit by dissipative pumping, Nat. Phys. **18**, 296 (2022).

[69] B. L. Brock, S. Singh, A. Eickbusch, V. V. Sivak, A. Z. Ding, L. Frunzio, S. M. Girvin, and M. H. Devoret, Quantum error correction of qudits beyond break-even, Nature (London) **641**, 612 (2025).

[70] M.-L. Cai, Y.-K. Wu, Q.-X. Mei, W.-D. Zhao, Y. Jiang *et al.*, Observation of supersymmetry and its spontaneous breaking in a trapped ion quantum simulator, Nat. Commun. **13**, 3412 (2022).

[71] C. Wang, Y. Y. Gao, P. Reinhold *et al.*, A Schrödinger cat living in two boxes, Science **352**, 1087 (2016).

[72] M. S. Winnel, J. J. Guanzon, D. Singh, and T. C. Ralph, Deterministic preparation of optical squeezed cat and Gottesman-Kitaev-Preskill states, Phys. Rev. Lett. **132**, 230602 (2024).

[73] T. Hillmann, F. Quijandría, G. Johansson, A. Ferraro, S. Gasparinetti, and G. Ferrini, Universal gate set for continuous-variable quantum computation with microwave circuits, Phys. Rev. Lett. **125**, 160501 (2020).

[74] S. Rosenblum, Y. Y. Gao, P. Reinhold *et al.*, A CNOT gate between multiphoton qubits encoded in two cavities, Nat. Commun. **9**, 652 (2018).

[75] S. Rosenblum, P. Reinhold, M. Mirrahimi, L. Jiang, L. Frunzio, and R. J. Schoelkopf, Fault-tolerant detection of a quantum error, Science **361**, 266 (2018).

[76] P. Reinhold, S. Rosenblum, W.-L. Ma, L. Frunzio, L. Jiang, and R. J. Schoelkopf, Error-corrected gates on an encoded qubit, Nat. Phys. **16**, 822 (2020).

[77] L. Hu, Y. Ma, W. Cai, X. Mu, Y. Xu *et al.*, Quantum error correction and universal gate set operation on a binomial bosonic logical qubit, Nat. Phys. **15**, 503 (2019).

[78] W. Wang, Z.-J. Chen, X. Liu *et al.*, Quantum-enhanced radiometry via approximate quantum error correction, Nat. Commun. **13**, 3214 (2022).

[79] C. Sayrin, I. Dotsenko, X. Zhou, B. Peaudecerf, T. Rybarczyk *et al.*, Real-time quantum feedback prepares and stabilizes photon number states, Nature (London) **477**, 73 (2011).

[80] S. Krastanov, M. Heuck, J. H. Shapiro, P. Narang, D. R. Englund, and K. Jacobs, Room-temperature photonic logical qubits via second-order nonlinearities, Nat. Commun. **12**, 191 (2021).